Selfconsistent Optimization of Molecular Geometries by Semi-empirical Force Field Method
II. Relaxational Effects Accompanying Torsion in Formamide*

Roman F. Nalewajski

Department of Theoretical Chemistry, Institute of Chemistry, Jagiellonian University, Krupnicza 41, 30-060 Kraków, Poland

(Z. Naturforsch. **32 a**, 276–284 [1977]; received January 3, 1977)

The geometry relaxation effects accompanying the internal rotation in formamide are investigated using the selfconsistent MINDO force field procedure [1]. The results of test calculations of H_2O_2 are also briefly summarized. The relaxation appears to be necessary for the barrier to the NH_2 inversion in formamide to be obtained. The calculated fully optimized equilibrium geometries of $CHONH_2$ and H_2O_2 are in good agreement with experiment. However, during the rotation geometry variations appear to be quite large. Application to formamide shows that torsion and inversion are strongly coupled. The nature of the barriers calculated is analyzed in terms of the MINDO energy partitioning. Finally, it is shown that the frozen-frame variations of the charges on atoms and dipole moment of formamide, are strongly affected by the geometry optimization during rotation.

1. Introduction

In recent years a number of calculations have been carried out on different molecules to investigate the geometry relaxation during internal rotation, i. e. the variation of molecular geometry together with the rotation angle of the barrier. In these works [2–16] the importance of geometry relaxation was pointed out. Although it has been shown that optimization of geometry can have a considerable effect on internal rotation barriers, it is usual to assume the hypothesis of the rigidity of the molecular skeleton during rotation, e. g. [17, 18]; the limited geometry optimization, without consideration of coupling between the geometrical parameters, is also sometimes introduced, e. g. [3, 11].

At the ab initio level the relaxed-frame type of calculations implies an important increase in the cost in comparison with the frozen-frame case [16]. So the complete geometry relaxation calculations on H_2O_2 only, the simplest molecule to exhibit an internal rotation, have been reported [2, 7, 9–11]. It follows from these calculations that geometry optimization is of great importance for a quantitative agreement with experiment to be reached; the crucial relaxational coordinate was found to be the OOH angle. By allowing the molecular skeleton to adjust itself to varying dihedral angle of H_2O_2 the cis barrier was substantially lowered.

In view of the qualitative success of semi-empirical SCF MO calculations in predicting the proper number of stable rotamers and approximate values for the potential barriers (see e. g. Ref. [17]) the relaxed-frame semi-empirical calculations have been performed on molecules possesing relatively large number of the relaxational degrees of freedom [4, 12–14]. It is emphasized in these works that the inclusion of geometry relaxation is sometimes necessary even for a qualitative agreement with experimental data, e. g. it has been shown that the rigidity of the biphenyl molecule during the rotation is the reason for the qualitative failure of the INDO method in predicting the torsional potential and the stable rotamers [4]. The recent report by Pancíř [12] indicates that geometry optimized CNDO/2 with configuration interaction predicts correctly the rotational dependence of the glyoxal energy.

Estimations of the geometry relaxation from the ab initio point of view have been obtained by fitting appropriate analytic functions to the calculated energies and locating the minima of those functions. Within standard semi-empirical theories, on the other hand, the quickly convergent force relaxational methods [1, 19–22] can be applied. The final relaxed geometry is sharply characterized in the force type calculations by vanishing forces on atoms, acting along the relaxational coordinates of a molecule. These forces can be calculated with negligible addi-

* Work presented in part at the Second International Congress of Quantum Chemistry, New Orleans, April 19–24, 1976.

Reprint requests to: Department of Chemistry, University of North Carolina, Chapel Hill, N.C. 27514, U.S.A., on leave from Jagiellonian University, Kraków.

tional computational expense. The efficient geometry optimization procedure has been developed by Dewar and his colleagues [23] for the case of MINDO/3 theory; within the classical conformational analysis the efficient optimization algorithms were proposed by Lifson and Warshel [24, 25] and by Sheraga and colleagues [26–28].

In a previous paper [1] we have investigated the convergence properties of the new force field optimization algirithm to be used to predict both the equilibrium and the saddle point geometries of molecular rotamers, based on the MINDO (CNDO, INDO) theory. As was pointed out there, the method converges very satisfactorily. It accounts for coupling between internal coordinates. In this paper, we consider the MINDO application of this method to geometry relaxation effects accompanying the torsion in formamide. The credibility of computational results is tested for the case of hydrogen peroxide. The changes in barrier components are discussed, the changes of the kinetic energy of valence electrons being estimated from the virial theorem. Emphasized are the effects of geometry relaxation on the various energy components in accordance with the MINDO (INDO) energy partitioning due to Dewar and Lo [29]. Special attention is paid to the changes of the net charges of atoms and dipole moment of formamide during rotation. The results are compared with experimental data where possible.

2. Method

The calculations have been caried out using the force field program, described in details in the previos paper [1], and the standard MINDO parametrization of Dewar and Lo [30], based on Oleari's method for the one centre integrals. The basis set was restricted to the valence shell Slater orbitals with the exponent of hydrogen 1 s orbital $\zeta_{1s}^{H} = 1.1$. Where optimized conformations are reported, they were obtained by letting the force field program run until the largest difference between a Cartesian nuclear coordinate and the corresponding coordinate resulting from the previous function recalculation was less than 0.005 Å.

Before discussing the results a few comments appear to be in order on the MINDO energy partitioning we have applied.

The total energy of a molecule, E, can be expressed as a sum of monocentric energy, E^{M}, and bicentric energy, E^{B},

$$E = E^{M} + E^{B} . \tag{1}$$

E^{M} and E^{B} can further be expanded in terms of contributions of various MINDO energy components [29]:

$$E^{M} = E_{U} + E_{ee}^{M} , \tag{2}$$

$$E^{B} = E_{R} + E_{V} + E_{ee}^{B} + E_{N} , \tag{3}$$

where

$$E_{ee}^{M} = E_{J}^{M} + E_{K}^{M} , \tag{4}$$

$$E_{ee}^{B} = E_{J}^{B} + E_{K}^{B} . \tag{5}$$

The one-electron terms, E_{U} and $(E_{R} + E_{V})$ represent the total one-centre and two-centre electron-core interaction energies respectively; E_{R} is the contribution of one-electron resonance integrals while E_{V} is the correction term in accordance with Goeppert-Mayer and Sklar approximation. E_{ee}^{M} and E_{ee}^{B} are the total one-centre and two-centre contributions to electron-electron repulsion energy; they can in turn be decomposed into corresponding Coulombic (J) and exchange (K) terms, familiar within the basic MO formalism. E_{N} means the core-core repulsion energy. Each of these one-centre and two-centre terms can be expressed as a sum of corresponding contributions from individual atoms and atomic pairs, respectively; for their explicit expressions the reader is referred to Reference 29.

Analysis of the barrier mechanisms from an energy standpoint is commonly used. The attractive-repulsive dominant theory [31, 32], based on the results of ab initio calculations, rest upon the energy partitioning

$$E = (T + V_{nn} + V_{ee}) + (V_{ne}) = (E_{rep}) + (E_{att}) , \tag{6}$$

where T is the kinetic energy, V_{nn} is the nucleus-nucleus repulsion energy, V_{ee} is the electron-electron repulsion energy, and V_{ne} is the electron-nucleus attraction energy. Barrier is classified to be attractive dominant, when $\Delta E_{att} > \Delta E_{rep}$, and to be repulsive dominant, when $\Delta E_{rep} > \Delta E_{att}$. The attractive and repulsive components of conformational barriers are very sensitive to the geometry optimization. So the only adequate classification in terms of this theory is that based on the completely optimized both the stationary and saddle point geometries.

In the case of semi-empirical all valence electron theories, like CNDO, INDO (MINDO) and NDDO, we cannot make the partition (6) directly, because the one-electron energy components E_{U} and E_{R} in-

clude both the kinetic and potential contributions, which are separately inaccessible

$$E_U = \sum_A [\sum_{u(A)} P_{uu} \langle u(1)| -\tfrac{1}{2}\Delta_1 + V_A(1)|u(1)\rangle] = \sum_A (\sum_{u(A)} P_{uu} U_{uu}) , \quad (7)$$

$$E_R = 2\sum_{A<B}\sum [\sum_{u(A)}\sum_{v(B)} P_{uv}\langle u(1)| -\tfrac{1}{2}\Delta_1 + V_A(1) + V_B(1)|v(1)\rangle] = 2\sum_{A<B}\sum [\sum_{u(A)}\sum_{v(B)} \beta_{AB} P_{uv}(I_u + I_v) S_{uv}] , \quad (8)$$

where subscripts A, B denote atoms in the molecule, u, v the running indexes of the valence shell atomic orbitals, P_{uv} is the charge and bond order matrix element, and symbol $V_X(k)$ denotes the potential energy operator of electron k interacting with the frozen core of atom X; U_{uu}, β_{AB}, I_u are the familiar MINDO parameters, while S_{uv} is the overlap integral. If one is interested only in energy differences between various conformations of the same molecule, the virial theorem can be used on purpose to estimate the change in the kinetic energy of valence electrons, ΔT, as the virial theorem in terms of the energy differences is expected to hold approximately within the frozen-core approximation,

$$2\Delta T + \Delta V + \Delta(\sum_A R_A \cdot \mathrm{grad}_{R_A} E) = 0 . \quad (9)$$

V is the change of the total potential energy of the valence electrons while R_A is the position vector of atom A.

3. Results

Geometry Relaxation

Table 1 presents the calculated structural data of the fully optimized equilibrium and saddle point geometries of H_2O_2 and $CHONH_2$. Figure 1 compares the calculated dependence of the hydrogen peroxide geometry on the dihedral angle, with that obtained by Dunning and Winter [2] from ab intio calculations. Effect of the internal rotation around the CN bond in formamide on structural parameters is visualized in Figure 3.

Table 1. Calculated structural data of the equilibrium and saddle point geometries of H_2O_2 and $CHONH_2$.

Conformer	Bond lengths (Å)			Angles (deg.)		
	Bond	Calcd	Obsd [a]	Angle	Calcd	Obsd [a]
Hydrogen peroxide:						
1) skewed	OO	1.340	1.475	HOO	115.1	94.8
	OH	1.145	0.950	HOOH [b]	109.3	111.5
2) cis	OO	1.338		HOO	117.7	
	OH	1.146		HOOH [b]	0.0	
3) trans	OO	1.330		HOO	114.1	
	OH	1.137		HOOH [b]	180.0	
Formamide [c]:						
1) equilibrium	CO	1.235	1.193	OCN	122.3	123.8
	CN	1.381	1.376	NCH	111.7	113.2
	CH	1.239	1.102	CNH′	122.8	117.2
	NH′	1.135	1.014	CNH″	121.2	120.6
	NH″	1.128	1.002	H′NH″	115.9	119.4
				α	6.14	6.123
				β	10.13	10.31
2) planar	CO	1.236		OCN	122.5	
	CN	1.378		NCH	112.0	
	CH	1.235		CNH′	122.6	
	NH′	1.126		CNH″	121.4	
	NH″	1.126		H′NH″	116.0	
3) twisted (90°)	CO	1.231		OCN	122.2	
	CN	1.439		NCH	111.4	
	CH	1.232		CNH	111.6	
	NH	1.147		HNH	101.0	
4) twisted (270°)	CO	1.227		OCN	119.7	
	CN	1.435		NCH	117.6	
	CH	1.249		CNH	116.5	
	NH	1.162		HNH	76.1	

[a] The experimental data for H_2O_2 were taken from Ref [34] and those for $CHONH_2$ from Ref. [33].
[b] Dihedral angle.
[c] See Figure 3.

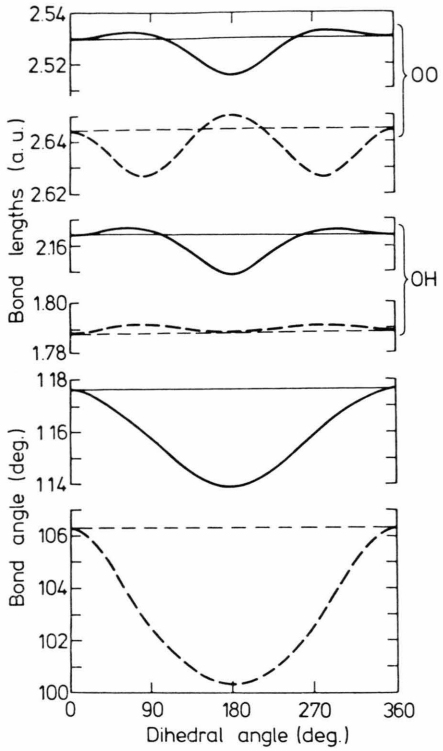

Fig. 1. Comparison of the MINDO (full line) and ab initio (broken line) variations of the geometrical parameters with dihedral angle for hydrogen peroxide. The ab initio curves were taken from Reference [2].

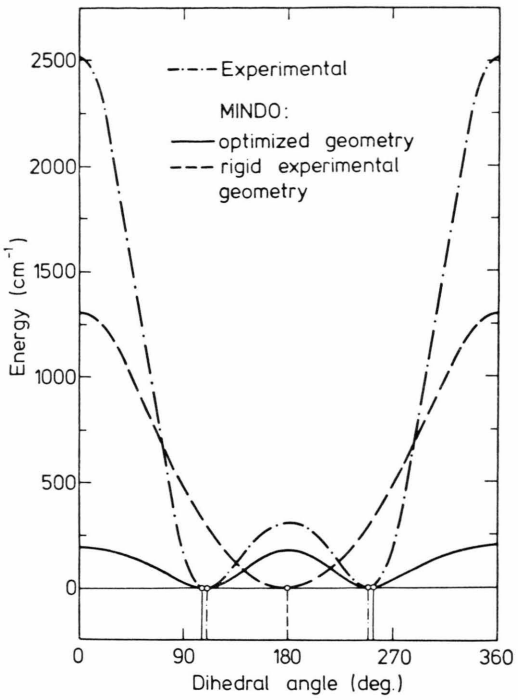

Fig. 2. Comparison of the MINDO geometrically optimized and unoptimized torsional potential energy curves for hydrogen peroxide with experimentally derived curve (taken from Reference [35]).

Barriers and Their Components

We have carried out calculations of the rotational barriers in hydrogen peroxide (treated as the test example) and in formamide, for both the relaxed-frame and frozen-frame variants. In addition the barrier to NH_2 inversion in formamide was also calculated. Results of these calculations are given in Table 2 and Figs. 2 and 4, where the effect of geometry relaxation on the barrier heights is shown. Changes of various barrier components, accompanying the internal rotation are summarized in Table 3. The total attractive and repulsive contributions to the calculated rotational barriers, obtained according to the frozen- and relaxed-frame calculations, are displayed in Table 4.

Dipole Moment and Net Charges of Atoms

It is clear that apart from energetic factors properties such as the dipole moment and net charges of atoms, which characterize the electron density distri-

Table 2. The effect of geometry optimization on the calculated barrier heights.

Molecule	Barrier [a]	Barrier height (kcal/mole) relaxed geometry	rigid geometry	Experimental	Ref.
Hydrogen peroxide	cis	0.531	2.999	7.04	35
	trans	0.484	−0.761	1.10	35
Formamide	$E(\varphi=90°)$ $-E(\varphi=0°)$	5.698	7.274	21.3	3
	$E(\varphi=270°)$ $-E(\varphi=180°)$	6.441	7.945		
	inversion	0.152	−1.196	1.058	33

[a] φ denotes angle of rotation.

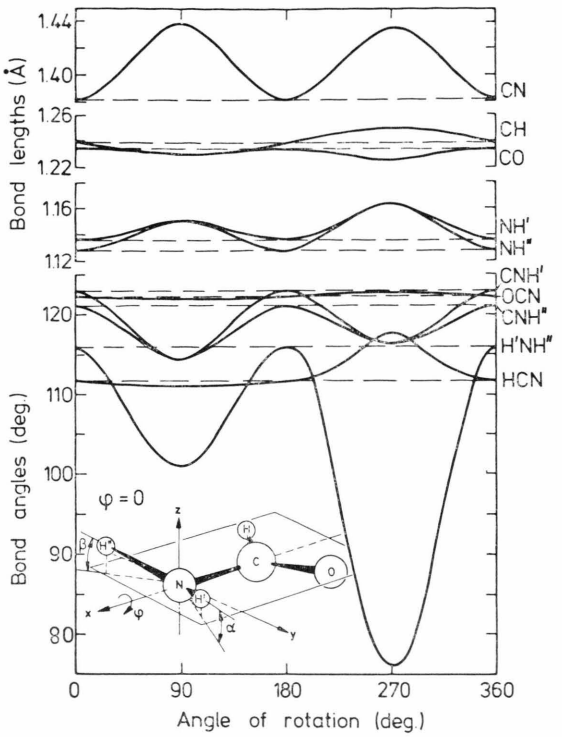

Fig. 3. The definitions of coordinate system and angle of rotation, φ, of NH_2 group in formamide, around the NC bond, and variations of geometrical parameters with angle of rotation. In the case of geometry optimization the torsional angle is defined to be zero when angles α and β, between the NCHO plane and the NH′ and NH″ bonds respectively, have their optimum values for the equilibrium formamide geometry (see Table 1): $\alpha=6.14°$, $\beta=10.13°$; the corresponding $\varphi=0°$ values for the case of rotation with the rigid experimental values of remaining structural parameters are: $\alpha=6.123°$, $\beta=10.31°$ (for the microwave structural parameters of formamide see Ref. [33]).

Table 3. Contributions (in eV) to the calculated barriers from different MINDO energy components [a], according to relaxed-frame calculations.

	Hydrogen peroxide		Formamide [b]	
	cis	trans	$E(\varphi=90°)-E(\varphi=0°)$	$E(\varphi=270°)-E(\varphi=180°)$
ΔE^{M}	0.044	0.251	−2.881	−4.418
ΔE_{U}	1.975	−1.538	−1.009	3.228
ΔE^{M}_{ee}	−1.931	1.788	−1.871	−7.647
ΔE^{M}_{J}	−2.221	2.071	−1.223	−7.187
ΔE^{M}_{K}	0.290	−0.283	−0.648	−0.460
ΔE^{B}	−0.020	−0.229	3.115	4.698
ΔE_{R}	−0.080	−0.525	3.298	4.392
ΔE_{V}	−0.514	−2.691	1.759	6.476
ΔE_{N}	−0.173	2.067	−1.655	−5.643
ΔE^{B}_{ee}	0.748	0.921	−0.281	−0.527
ΔE^{B}_{J}	0.788	0.855	−0.484	−0.929
ΔE^{B}_{K}	−0.040	0.066	0.199	0.402

[a] See text. [b] φ denotes angle of rotation.

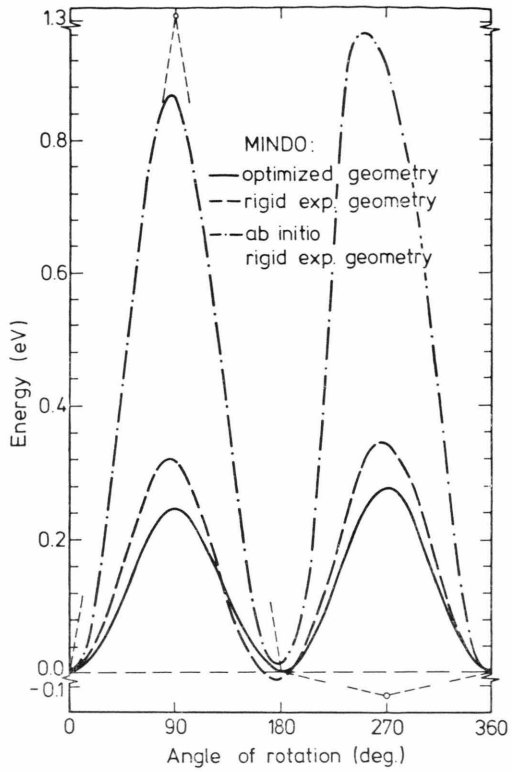

Fig. 4. Comparison of the MINDO geometrically optimized and unoptimized torsional potential energy curves for formamide with the ab initio frozen frame curve (from Ref. [3]). Points ° refer to calculations with the structural parameters the same as for experimental geometry, except for angles $CNH'=CNH''=N'NH''=109.45°$ (the sp^3 hybridization on nitrogen atom for the $\varphi=90°$ and $\varphi=270°$ rotamers).

bution in a molecule, will be quite sensitive to variations in geometry due to relaxation. Such an analysis has been performed for formamide, and its results are shown in Table 5 and in Figs. 5 – 7, where displayed also are the extra changes of these properties due to geometry optimization.

4. Discussion

Hydrogen peroxide

It follows from the ab initio calculations on H_2O_2 by Dunning and Winter [2] that geometry optimization play an important role for cis barrier, having, on the other hand, a little effect on the trans barrier. The changes of geometrical parameters with dihedral angle derived from these calculations are compared with the present MINDO results in Figure 1. It can be seen that the present work MINDO equilibrium

Table 4. The total attractive and repulsive components of the calculated rotational barriers.

Molecule	Barrier [a]	Rotation [b]	Barrier components (in eV) ΔT	ΔE_{rep} [c]	ΔE_{att} [d]
Hydrogen peroxide:	cis	F	−0.128	0.767	−0.639
		R	−0.024	−1.380	1.405
	trans	R	−0.023	4.753	−4.731
Formamide	$E(\varphi=90°)-E(\varphi=0°)$	F	−0.316	−0.776	1.091
		R	−0.592	−4.403	4.640
	$E(\varphi=270°)-E(\varphi=180°)$	F	−0.365	−3.229	3.596
		R	−0.133	−13.954	14.233

[a] φ denotes angle of rotation.
[b] The symbols F and R denote the frozen- and relaxed-frame cases, respectively.
[c] $\Delta E_{rep}=\Delta T+\Delta E^{M}_{ee}+\Delta E^{B}_{ee}+\Delta E_{N}$.
[d] $\Delta E_{att}=\Delta E_{U}+\Delta E_{R}-\Delta T+\Delta E_{V}$.

geometry is in semiquantitative agreement with experiment. Figure 1 gives an idea how realistic MINDO geometry relaxation effects are. It can be seen that except for the different behaviour of the OO distance variations the predicted MINDO dependencies of structural parameters on the dihedral angle agree qualitatively, but not quantitatively, with those for the ab initio case.

The rigid rotation calculations do not predict any trans barrier. The relaxed-frame variant, on the other hand, leads to the qualitatively correct curve, with the minimum energy dihedral angle predicted to be very close to the experimental value. While reproducing the trans barrier quite satisfactorily, these calculations greatly underestimate the cis barrier wich is predicted to be almost equal to the trans barrier. A similar approximate equality was found within the INDO theory by England and Gordon [15]. Reasons for this are not clear, but we expect it is due to the poor representation of the lone pair effects within the INDO (MINDO) theory. The geometry optimization affects much various barrier components. The corresponding changes predicted within the relaxed-frame variant are listed in Table 3; they agree qualitatively with the values reported previously [6, 15].

Formamide

Formamide has been examined quite extensively by a number of theoretical approaches as being the simplest model for the peptide bond. The rigid

Table 5. Comparison of the MINDO and ab initio [a] dipole moments (in Debye units) of formamide rotamers.

Rotation angle φ (deg.)	Remaining structural parameters [c]	Method	$-\mu_x$	μ_y	μ_z	μ_{total}
0	Experimental	MINDO	3.432	3.441	−1.003	4.962
		ab initio	4.236	2.837	−0.534	4.138
		exptl [d]	2.410	2.828		
	Optimized	MINDO	3.651	3.643	−0.961	5.246
		ab initio [f]	3.115	2.959	−0.529	4.929
90	Experimental	MINDO	2.771	2.074	0.107	3.463
		ab initio	2.325	1.891	0.050	2.997
	Optimized	MINDO	1.856	0.022	0.000	1.856
270	Experimental	MINDO	2.732	4.278	−0.110	5.077
	Optimized	MINDO	1.493	7.136	0.000	7.290
0	Exptl (except $\alpha=\beta=0°$) [e]	MINDO	1.939	4.792	0.000	5.169
		ab initio	3.018	2.869	0.000	4.164
	Optd (except $\alpha=\beta=0°$) [e]	MINDO	1.745	5.052	0.000	5.345

[a] Ref. [3], frozen-frame calculations (no d functions).
[b] For the definitions of angles and coordinate system see Figure 3.
[c] For the experimental structural data see Reference [33].
[d] Reference [36]. [e] Planar model. [f] Partly optimized geometry.

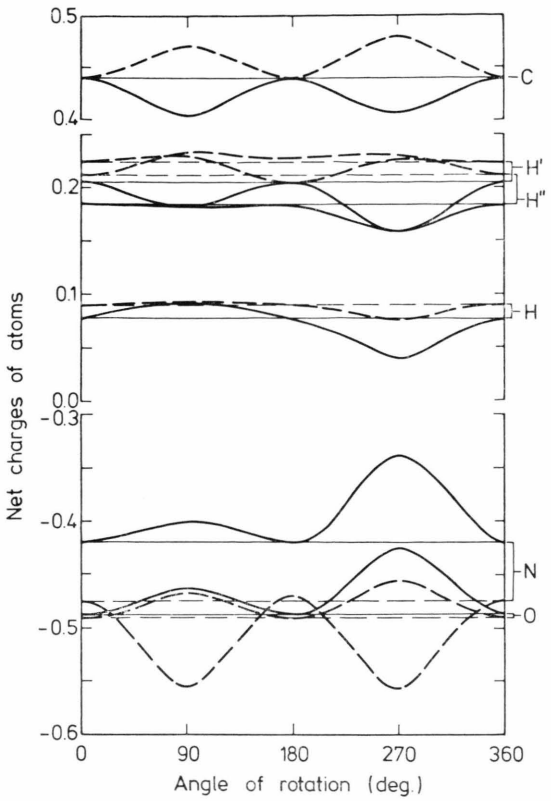

Fig. 5. Net charges of atoms in formamide as a function of rotation angle. The full line curves refer to optimized geometries while the broken line curves refer to the rigid experimental skeleton during rotation.

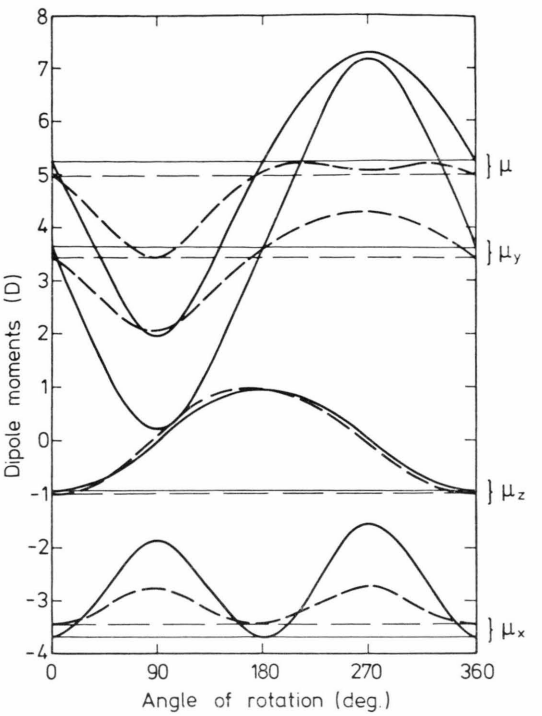

Fig. 6. The total dipole moment of formamide, and its components as a function of rotation angle. The full line and broken line curves refer to the calculations with and without geometry optimization during rotation respectively. For the definition of the coordinate system see Figure 3.

rotation estimates of the barrier to internal rotation have been made, both from semi-empirical [37] and ab initio (see e. g. Ref. [3]) points of view, giving a semiquantitative agreement with experiment. The present calculations were undertaken in order to determine how the inclusion of the complete coupling between geometrical parameters during the geometry relaxation alters the predicted structural, energetical and charge distribution factors as a functions of the rotation angle.

The predicted nonplanar equilibrium geometry (Table 1) is in remarkably good agreement with the known gas phase structure [33], with out of plane nonequivalent bending of the two NH bonds. The present calculations reproduce the structural parameters better than the recently reported STO-3G calculations by Daudey [38]. It should be noted, that the frozen-frame calculations fail to give the correct sign of the inversion barrier, predicting the ground state geometry to be planar.

The main predicted geometry relaxation effects, summarized in Fig. 3 and in Table 1, are consistent with the qualitative expectations: a) the CN bond lengthening in the $\varphi = 90^\circ$ and $\varphi = 270^\circ$ rotamers,

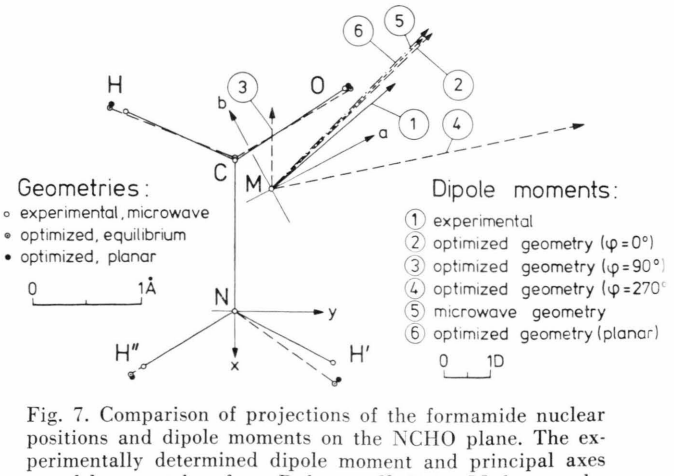

Fig. 7. Comparison of projections of the formamide nuclear positions and dipole moments on the NCHO plane. The experimentally determined dipole moment and principal axes a and b were taken from Reference [36]. Point M denotes the centre of mass of the experimental formamide geometry, projected on the NCHO plane.

due to loss of a partly double bond character: b) approximate constancy of the OCN angle, due to unchanged sp^2 hybridization on carbon atom during rotation; c) a remarkable decrease of the HNH and CNH bond angles in the $\varphi = 90^\circ$ and $\varphi = 270^\circ$ conformers, owing to expected change of hybridization on nitrogen in both transition states; d) the small decrease of HCN bond angle for $\varphi = 90^\circ$ and its increase for $\varphi = 270^\circ$, due to repulsive interaction between the H atom and rotating H′ and H″ atoms.

Geometry optimization shows that the amine group undergoes partial inversion in stationary positions. This result, similar to that reported by Payne for methylamine [16], shows that there is strong coupling between inversion and torsion of the amine group.

The question naturally arises: how realistic the predicted semiempirical geometry variations are? The comparison with the corresponding relaxed-frame ab initio calculations is not presently possible. Among the results we have obtained the most striking effect is certainly the large difference between the optimum values of HNH bond angle for $\varphi = 90^\circ$ and $\varphi = 270^\circ$ respectively ($\sim 25^\circ$).

Table 2 and Fig. 4 demonstrate that the predicted torsional potential curves are again too flat. We hope, that a new set of MINDO parameters, derived within the relaxed-frame model of internal rotation, will improve the quantitative agreement with experiment.

Figure 4 shows that the consideration of the limited bond angle relaxation by assuming the sp^3 hybridization on nitrogen for $\varphi = 90^\circ$ and $\varphi = 270^\circ$ (this actually reflects the general trends in variations of the CNH and HNH bond angles), fails to predict the $\varphi = 270^\circ$ barrier. This result shows the importance of the simultaneous optimization of all geometrical parameters for the qualitatively correct results to be obtained.

It follows from Table 4 that both barriers are classified as being attractive dominant. Geometry relaxation having a large effect on individual barrier components does not alter these characters.

It is of interest to note that the geometry relaxation changes qualitatively the behaviour of the variations of the net charges on the C, N, H′ and H″ atoms (Fig. 5), giving as a result the large differences in the calculated dipole moments (see Fig. 6 and Table 5). Thus a great care should be taken in use the frozen-frame charges for the interpretation of the charge density variations accompanying the internal rotation. Figure 5 demonstrates the general trend in the net charge variation, originating from the geometry relaxation: the relaxed-frame calculations lead to a more smooth charge distributions than that for the frozen-frame case. Note that variations of charges on atoms, which appear as the $\varphi = 90^\circ$ and $\varphi = 270^\circ$ barriers are crossed, are very similar when rotation is of rigid type. This similarity is significantly perturbed after geometry relaxation: charges on atoms are much more reduced for the $\varphi = 270^\circ$ than those for $\varphi = 90^\circ$.

A general conclusion from Figs. 6 and 7, and from Table 5 is that the dipole moments calculated for $\varphi = 0^\circ$ microwave and fully optimized geometries, respectively, are almost the same. The total $\varphi = 0^\circ$ dipole moments are overestimated within MINDO parametrization we have used, but their directions are in good agreement with experiment. However, a significantly different results have been obtained for the transition state conformers. Since we expect the changes for larger molecular systems to be still more important, the usual procedure of determination of the dipole moment changes during the internal rotation, based on he frozen-frame type calculations (see e. g. Ref. [37]) is clearly erroneous.

The work was supported by the Institute of Low Temperatures and Structural Research, Polish Academy of Sciences, Wrocław.

The author would like to thank to Professor A. Gołębiewski for his continuous interest in the problem and helpful discussions. The computer time was provided by the Jagiellonian University Computer Centre.

[1] R. F. Nalewajski, J. Mol. Structure, accepted for publication.
[2] T. H. Dunning and N. W. Winter, J. Chem. Phys. **63,** 1847 [1975].
[3] D. H. Christensen, R. N. Kortzeborn, B. Bak, and J. J. Led, J. Chem. Phys. **53,** 3912 [1970].
[4] J. C. Rayez and J. J. Dannenberg, Chem. Phys. Letters, submitted for publication.
[5] O. Sovers and M. Karplus, J. Chem. Phys. **44,** 3033 [1966].
[6] M. S. Gordon, J. Amer. Chem. Soc. **91,** 3122 [1969].
[7] A. Veillard, Chem. Phys. Letters **4,** 51 [1969].
[8] I. R. Epstein and W. N. Lipscomb, J. Amer. Chem. Soc. **92,** 6094 [1970].
[9] R. B. Davidson and L. C. Allen, J. Chem. Phys. **55,** 519 [1971].

[10] J. P. Ranck and H. Johansen, Theoret. Chim. Acta **24,** 334 [1972].
[11] O. Gropen and H. H. Jensen, J. Mol. Structure **32,** 85 [1976].
[12] J. Pančíř, Theoret. Chim. Acta **40,** 81 [1975].
[13] M. J. S. Dewar and M. C. Kohn, J. Amer. Chem. Soc. **94,** 2699 [1972]
[14] W. England and M. S. Gordon, J. Amer. Chem. Soc. **93,** 4699 [1971].
[15] W. England and M. S. Gordon, J. Amer. Chem. Soc. **94,** 4818 [1972].
[16] P. W. Payne, J. Chem. Phys. **65,** 1920 [1976].
[17] E. L. Wagner, Theoret. Chim. Acta **23,** 115, 127 [1971].
[18] C. Guidotti, U. Lamanna, M. Maestro, and R. Moccia, Theoret. Chim. Acta **27,** 55 [1972].
[19] R. F. Nalewajski and A. Gołębiewski, Acta Phys. Polon. **A 49,** 689 [1976].
[20] J. W. McIver and A. Komornicki, Chem. Phys. Letters **10,** 303 [1971]; J. Amer. Chem. Soc. **94,** 2625 [1972]; **95,** 4512 [1973].
[21] P. Pulay and F. Török, Mol. Phys. **25,** 153 [1973].
[22] J. Pančíř, Theoret. Chim. Acta **29,** 21 [1973]; Collect. Czech. Chem. Commun. **40,** 1112, 2726 [1975].
[23] R. Ch. Bingham, M. J. S. Dewar, and D. H. Lo, J. Amer. Chem. Soc. **97,** 1285 [1975].
[24] S. Lifson and W. Warshel, J. Chem. Phys. **49,** 5116 [1968].
[25] A. Warshel and S. Lifson, J. Chem. Phys. **53,** 582 [1970].
[26] R. A. Scott and H. A. Scheraga, J. Chem. Phys. **45,** 2091 [1966].
[27] H. A. Scheraga, Adv. Phys. Org. Chem. **6,** 103 [1968].
[28] L. I. Shipmann, A. W. Burgess, and A. A. Scheraga, Proc. Natl. Acad. Sci. (USA) **72,** 543 [1975].
[29] M. J. S. Dewar and D. H. Lo, J. Amer. Chem. Soc. **93,** 7201 [1971].
[30] M. J. S. Dewar and D. H. Lo, J. Amer. Chem. Soc. **94,** 5296 [1972].
[31] L. C. Allen, Chem. Phys. Letters **2,** 597 [1968].
[32] W. L. Jorgensen and L. C. Allen, J. Amer. Chem. Soc. **93,** 567 [1971].
[33] C. C. Costain and J. M. Dowling, J. Chem. Phys. **32,** 158 [1960].
[34] R. L. Redington, W. B. Olson, and P. C. Cross, J. Chem. Phys. **36,** 1311 [1962].
[35] R. H. Hunt, R. A. Leacock, C. W. Peters, and K. T. Hecht, J. Chem. Phys. **42,** 1931 [1965].
[36] R. J. Kurland and E. B. Wilson, J. Chem. Phys. **27,** 585 [1957].
[37] J. F. Yan, F. A. Momany, R. Hoffmann, and H. A. Scheraga, J. Amer. Chem. Soc. **74,** 420 [1970].
[38] J. P. Daudey, the fully optimized equilibrium geometry reported in: M. A. Armbruster and A. Pulman, FEBS Letters **49,** 18 [1974].
[39] J. E. Rabinovitch, J. E. Douglas, and F. S. Looney, J. Chem. Phys. **20,** 1807 [1952].